

Constraints on cosmological parameters from Planck and BICEP2 data

Luis A. Anchordoqui

*Department of Physics and Astronomy,
Lehman College, City University of New York, Bronx NY 10468, USA*

Abstract. We show that the tension introduced by the detection of large amplitude gravitational wave power by the BICEP2 experiment with temperature anisotropy measurements by the Planck mission is alleviated in models where extra light species contribute to the effective number of relativistic degrees of freedom. We also show that inflationary models based on S -dual potentials are in agreement with Planck and BICEP2 data.

1. Fitting Λ CDM + r to Planck and BICEP2 data

Measurements of the cosmic microwave background (CMB) and large scale structure (LSS) indicate that we live in a spatially-flat, accelerating, infinite universe composed of 4% of baryons (b), 26% of (cold) dark matter (CDM), and 70% of dark energy (Λ). These observations also reveal that the universe has tiny ripples of adiabatic, scale-invariant, Gaussian density perturbations. The favored Λ CDM model implicitly includes the hypothesis of a very early period in which the scale factor of the universe expands exponentially: $a \propto e^{Ht}$, where $H = \dot{a}/a$ is the Hubble parameter (see e.g. Baumann 2009). If the interval of exponential expansion satisfies $\Delta t > N/H$, with N above about 50 to 60, a small casually connected region can grow sufficiently to accommodate the observed homogeneity and isotropy, to dilute any overdensity of magnetic monopoles, and to flatten the spatial hyper-surfaces (i.e., $\Omega \equiv \frac{8\pi\rho}{3M_{\text{PL}}H^2} \rightarrow 1$, where $M_{\text{PL}} = G^{-1/2}$ is the Planck mass and ρ the energy density; throughout we use natural units, $c = \hbar = 1$). Quantum fluctuations during this inflationary period can explain the observed cosmological perturbations.

Fluctuations are created quantum mechanically on subhorizon scales with a spectrum of wavenumbers k . (A mode k is called superhorizon when $k < aH$ and subhorizon when $k > aH$.) While comoving scales, k^{-1} , remain constant the comoving Hubble radius, $(aH)^{-1}$, shrinks quasi-exponentially during inflation (driving the universe toward flatness) and the perturbations exit the horizon. Causal physics cannot act on superhorizon perturbations and they freeze until horizon re-entry at late times. A mode exiting the horizon can then be described

by a classical probability distribution with variance given by the power spectrum $\mathcal{P}_\chi(k)$. After horizon re-entry the fluctuations evolve into anisotropies in the CMB and perturbations in the LSS. The scale-dependence of the power spectrum is defined by the scalar spectral index, $n_s - 1 \equiv d \ln \mathcal{P}_\chi / d \ln k$, and its running $\alpha_s \equiv dn_s / d \ln k$. The power spectrum is often approximated by a power law form: $\mathcal{P}(k) = A_s(k_*) (k/k_*)^{n_s - 1 + \frac{1}{2}\alpha_s \ln(k/k_*) + \dots}$, where k_* is an arbitrary reference that typifies scales probed by the CMB.

The Planck temperature spectrum at high multipoles ($l \gtrsim 40$) describes the standard spatially-flat Λ CDM 6-parameter model $\{\Omega_b h^2, \Omega_{\text{CDB}} h^2, \Theta_s, \tau, n_s, A_s\}$ with high precision: (i) baryon density, $\Omega_b = 0.02207 \pm 0.00033$; (ii) CDM density, $\Omega_{\text{CDM}} h^2 = 0.1196 \pm 0.0031$; (iii) angular size of the sound horizon at recombination, $\Theta_s = (1.04132 \pm 0.00068) \times 10^{-2}$; (iv) Thomson scattering optical depth due to reionization, $\tau = 0.097 \pm 0.038$; (v) scalar spectral index, $n_s = 0.9616 \pm 0.0094$; (vi) power spectrum amplitude of adiabatic scalar perturbations, $\ln(10^{10} A_s) = 3.103 \pm 0.072$ (Ade et al. 2013a). Planck data also constrain the Hubble constant $h = 0.674 \pm 0.012$ and $\Omega_\Lambda = 0.686 \pm 0.020$. (Herein we adopt the usual convention of writing the Hubble constant at the present day as $H_0 = 100 h \text{ km s}^{-1} \text{ Mpc}^{-1}$.) Note, however, that the data only measure accurately the acoustic scale, and the relation to underlying expansion parameters (e.g., via the angular-diameter distance) depends on the assumed cosmology, including the shape of the primordial fluctuation spectrum. Even small changes in model assumptions can change h noticeably. Unexpectedly, the H_0 inference from Planck data deviates by more than 2σ from the previous result from the maser-cepheid-supernovae distance ladder $h = 0.738 \pm 0.024$ (Riess et al. 2011). The impact of the Planck h estimate is particularly important in the determination of the number of “equivalent” light neutrino species: N_{eff} (Steigman et al. 1977). Combining observations of the CMB with data from baryon acoustic oscillations (BAO), the Planck Collaboration reported $N_{\text{eff}} = 3.30 \pm 0.27$ (Ade et al. 2013b). However, if the value of h is not allowed to float in the fit, but instead is frozen to the value determined from the maser-cepheid-supernovae distance ladder the Planck CMB data then gives $N_{\text{eff}} = 3.62 \pm 0.25$, which suggests new neutrino-like physics (at around the 2.3σ level).

Inflation also produces fluctuations in the tensor part of the spatial metric. The gravity-wave fluctuations are also frozen on super-horizon scales and their B -mode power spectrum, $\mathcal{P}_h = A_t \left(\frac{k}{k_*}\right)^{n_t + \frac{1}{2}\alpha_t \ln\left(\frac{k}{k_*}\right) + \dots}$, can be imprinted in the CMB temperature and polarization. We define the tensor-to-scalar amplitude ratio $r = A_t/A_s$ as the free parameter for the Λ CDM + r model.

As the BICEP2 Collaboration carefully emphasized (Ade et al. 2014), the measurement of $r = 0.2_{-0.05}^{+0.07}$ (or $r = 0.16_{-0.05}^{+0.06}$ after foreground subtraction, with

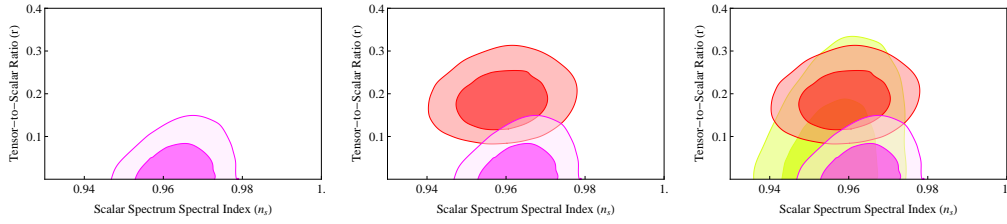


Figure 1. Marginalized joint 68% CL and 95% CL regions for (r, n_s) using Planck + WMAP + BAO data without a running spectral index (left), BICEP2 data with $\alpha_s \neq 0$ (middle), and Planck + WMAP + BAO data with $\alpha_s \neq 0$ (right).

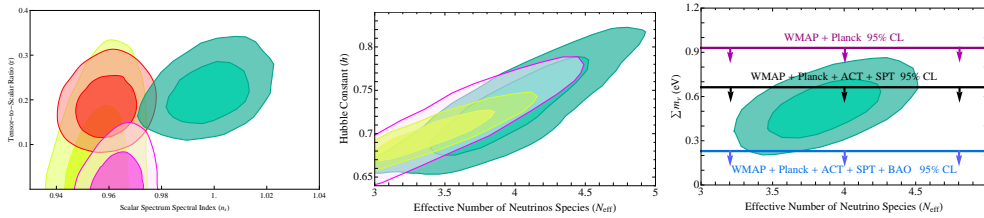


Figure 2. *Left:* Marginalized joint 68% CL and 95% CL regions for (r, n_s) using Planck + WMAP + BAO with and without a running spectral index, BICEP2 data with $\alpha_s \neq 0$ and allowed regions of the 9-parameter fit. *Middle:* 68% and 95% confidence regions for Λ CDM + N_{eff} , using Planck + WMAP (pink) and Planck + WMAP + BAO (yellow) data, together with allowed regions of the 9-parameter fit (green) together. *Right:* 68% and 95% confidence regions of the 9-parameter fit. The horizontal lines indicate the 95% CL upper limits on $\sum m_\nu$.

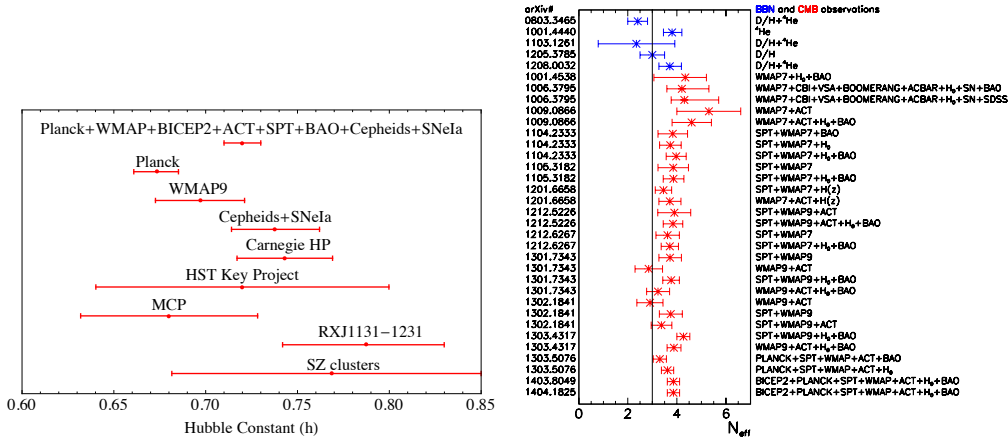


Figure 3. Recent H_0 (left) and N_{eff} (right) measurements and the 1σ confidence intervals from various combinations of models and data sets.

$r = 0$ disfavored at 5.9σ) from the B-mode polarization appears to be in tension with the 95% CL upper limits reported by the WMAP ($r < 0.13$, Hinshaw et al. 2009) and Planck ($r < 0.11$, Ade et al. 2013a) collaborations from the large-scale CMB temperature power spectrum. As shown in Fig. 1, extension of the 7-parameter model to include non-zero running of the spectral index ameliorates the tension. However, the combination of Planck and BICEP2 data favors $\alpha_s < 0$ at almost the 3σ level, with best fit value around $\alpha_s = -0.028 \pm 0.009$ (68%CL) (Ade et al. 2014). This is about 100 times larger than single-field (ϕ) inflation would predict. Such a particular running can be accommodated, however, if V''' / V is roughly 100 times larger than the natural expectation from the size of $V' / V \sim (10M_{\text{Pl}})^{-1}$ and $V'' / V \sim (10M_{\text{Pl}})^{-2}$, where $V(\phi)$ is the inflaton potential (Smith et al. 2014). In Fig. 2 we compare the aftermath of the multiparameter fit of $\{\Omega_b h^2, \Omega_{\text{CDB}} h^2, \Theta_s, \tau, n_s, A_s, r, N_{\text{eff}}, \sum m_\nu\}$ to the data reported by the Planck and BICEP2 collaborations (Dvorkin et al. 2014; Anchordoqui et al. 2014a). Clearly, a higher effective number of relativistic species can relieve the tension between Planck and BICEP2 results. As shown in Fig. 3, the best multiparameter fit yields $N_{\text{eff}} = 0.81 \pm 0.25$ and $h = 0.70 \pm 0.01$, which are consistent with previous measurements.

We end with an observation: that one should keep in mind that there is an on going controversy concerning the effect of background on the BICEP2 result (Liu et al. 2014; Flauger et al. 2014). In the next section we play devil’s advocate and assume that the BICEP2 results are flawed.

2. S -dual Inflation

Planck data favor standard slow-roll single field inflationary models with plateau-like potentials $V(\phi)$ for which $V'' < 0$, over power-law potentials. However, most of these plateau-like inflaton potentials experience the so-called “unlikeliness problem” (Ijjas et al. 2013). The requirement that $V'' < 0$ in the de Sitter region, and the avoidance of the unlikeliness problem, must now also accommodate (if possible) the tensor-to-scalar ratio detected by BICEP2 data. Finally, a wish rather than a constraint: that the inflaton potential possess some connection to particle physics. To this end, we hypothesize that the potential be invariant under the S -duality constraint $g \rightarrow 1/g$, or $\phi \rightarrow -\phi$, where ϕ is the dilaton/inflaton, and $g \sim e^{\phi/M}$.¹ Here M is expected to be within a

¹String theory exhibits various forms of dualities, i.e. relation between different theories at large and small radii of the compactified manifold (target space duality, or T duality, Giveon et al. 1994) and at strong and weak coupling (S duality, Font et al. 1990). At the classical level, these dualities appear in equations of motion and in their solutions. Herein we do not attempt

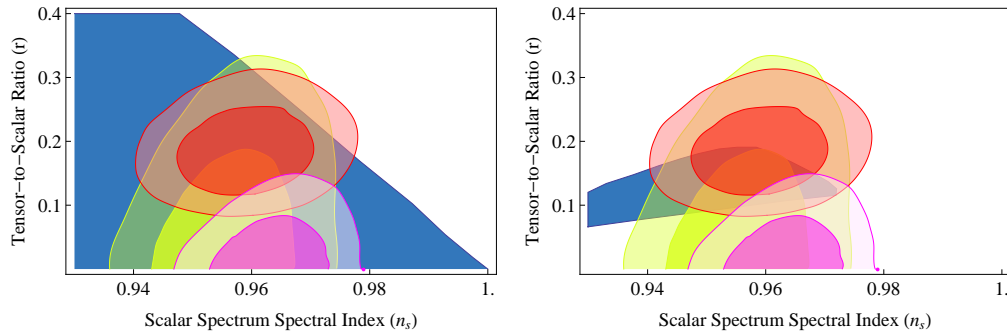


Figure 4. Available parameter space to the potential V_1 (left) and V_2 (right) together with favored regions by Planck and BICEP2 data (Anchordoqui et al. 2014b). For V_2 , $N > 60$ corresponds to $r \lesssim 0.1$

few orders of magnitude of M_{Pl} . This requirement forces the functional form $V(\phi) = f[\cosh(\phi/M)]$ on the potential. In what follows we take for V the S self-dual form $V_1 = V_0 \text{sech}(\phi/M)$, and $V_2 = V_0 [\text{sech}(3\phi/M) - \frac{1}{4}\text{sech}^2(\phi/M)]$, which solve the unlikeliness problem because they have no power-law wall. For V_1 , as for power-law inflation (with an exponential potential), inflation does not end. We assume that the dynamics of a second field leads to exit from the inflationary phase into the reheating phase. The requirement that there be 50 to 60 e -folds of observable inflation yields $M \gtrsim 1.4M_{\text{Pl}}$, constraining the available region in the $r - n_s$ plane. As can be seen in Fig. 4, the allowed region is consistent with both Planck and BICEP2 data. (Details of the calculation are given in Anchordoqui et al. 2014b). However, as anticipated above, the prediction for α_s is about 100 times smaller than the observed 68% confidence regions, see Fig. 5. For $\alpha_s \neq 0$, agreement with data is only attained at 95% CL.

Acknowledgments. I thank my collaborators Vernon Barger, Haim Goldberg, Xing Huang, Danny Marfatia, and Brian Vlcek for their contributions to the work discussed here. This work has been supported by the U.S. NSF CAREER Award PHY-1053663 and by NASA Grant No. NNX13AH52G.

References

- Ade, P.A.R., et al. [BICEP2 Collaboration] 2014, PhRvL, **112**, 241101.
 Ade, P.A.R., et al. [Planck Collaboration] 2013a, arXiv:1303.5082.
 Ade, P.A.R., et al [Planck Collaboration] 2013b, arXiv:1303.5076.

a full association with a particular string vacuum, but simply regard the self-dual constraint as a relic of string physics in big bang cosmology.

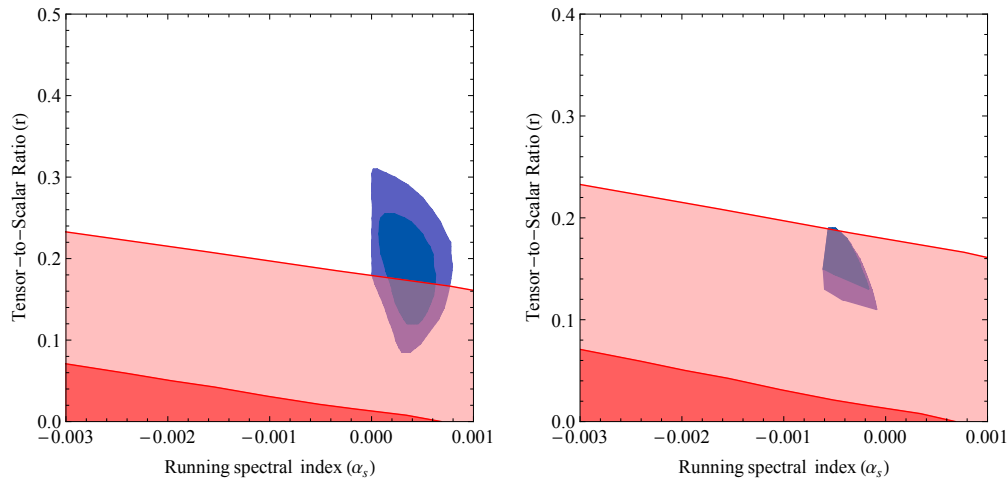


Figure 5. The blue regions show the predictions of α_2 for the parameter space available to V_1 (left) and V_2 (right) after fixing r to be within the 68% and 95% CL regions of BICEP2 measurements. The red areas show the 68% and 95% CL regions favored by a combination of Planck data, WMAP polarization data and small scale CMB data (Ade et al. 2013a).

Anchordoqui, L.A., Goldberg, H., Huang, X., & Vlcek B.J. 2014a, JCAP, **1406**, 042.

Anchordoqui, L.A., Barger, V., Goldberg, H., Huang, X., & Marfatia, D. 2014b, PhLB, **734**, 134.

Baumann, D. 2009, arXiv:0907.5424.

Dvorkin, C., Wyman, M., Rudd, D.H., & Hu, W. 2014, arXiv:1403.8049

Flauger, R., Hill, J.C., & Spergel, D.N. 2014, arXiv:1405.7351.

Font, A., Ibáñez, L.E., Lüst, D., & Quevedo, F. 1990, PhLB, **249**, 35.

Giveon, A., Porrati, M., & Rabinovici, E. 1994, PhR, **244**, 77.

Hinshaw, G., et al. [WMAP Collaboration] 2013, ApJS, **208**, 19.

Ijjas, A., Steinhardt, P.J., & Loeb, A. 2013, PhLB, **723**, 261.

Liu, H., Mertsch, P., & Sarkar, S. 2014, ApJ, **789**, L29.

Riess, A.G., et al. 2011, ApJ, **730**, 119. [Erratum-ibid. **732**, 129, (2011)].

Smith, K.M., Dvorkin, C., Boyle, L., Turok, N., Halpern, M., Hinshaw, G., & Gold, B. 2014, PhRvL, **113**, 031301.

Steigman, G., Schramm, D.N., & Gunn, J.E. 1977, PhLB **66**, 202.